Visual Comput (2006)
DOI 10.1007/s00371-006-0011-9

ORIGINAL ARTICLE

Tomoyuki Nieda
Alexander Pasko
Tosiyasu L. Kunii

Detection and classification of topological evolution for linear metamorphosis

T. Nieda (✉) · A. Pasko
Graduate School of Computer and Information Sciences, Hosei University, 3-7-2 Kajino-cho Koganei-shi, Tokyo 184-8584, Japan
i04t0013@cis.k.hosei.ac.jp,
pasko@k.hosei.ac.jp

A. Pasko · T.L. Kunii
IT Institute, Kanazawa Institute of Technology, 1-15-13 Jingumae, Shibuya-ku, Tokyo 150-0001 Japan
tosi@kunii.com

Abstract The advantage of functional methods for shape metamorphosis is the automatic generation of intermediate shapes possible between the key shapes of different topology types. However, functional methods have a serious problem: shape interpolation is applied without topological information and thereby the time values of topological changes are not known. Thus, it is difficult to identify the time intervals for key frames of shape metamorphosis animation that faithfully visualize the topological evolution. Moreover, information on the types of topological changes is missing. To overcome the problem, we apply topological analysis to functional linear shape metamorphosis and classify the type of topological evolution by using a Hessian matrix. Our method is based on Morse theory and analyzes how the critical points appear. We classify the detected critical points into maximum point, minimum point, and saddle point types. Using the types of critical points, we can define the topological information for shape metamorphosis. We illustrate these methods using shape metamorphosis in 2D and 3D spaces.

Keywords Critical point classification · Morse theory · Shape metamorphosis · Topological evolution

1 Introduction

Transformation of one given shape into another is called *metamorphosis* or morphing. Shape metamorphosis animations are widely used in several fields, such as movies, TV commercials, and games. Metamorphosis brings about stunning visual effects especially when *topological evolutions* are involved.

There are many known techniques of shape metamorphosis [6]. Some of them utilize topological information. For example, Pizzanu et al. [5] proposed a method using the Reeb graph and contours of input objects. There are two major types of shape metamorphosis techniques: polygon-based methods and function-based methods. A polygon-based method has some problems, such as establishing correspondence and interpolation. The correspondence defines which point of the initial geometry corresponds to which point of the target geometry, and the vertex path (interpolation) defines the way each point reaches its destination. Hence, it is difficult for polygon-based methods to apply shape metamorphosis between key shapes of different topology. The definition of topological information is required for shape metamorphosis between objects of different topology. The so-called *topological handles* are required for defining the topological information. These handles show how the topology changes, and appear or vanish before and after the topological evolution. Therefore, the handles are embedded when the topology of the polyhedral shapes changes. The techniques based on topological handles appeared in [2, 9].

Apart from the topological handle approach, there is a skeletal implicit surfaces approach: Galin et al. [3] proposed a shape metamorphosis based on Minkowski sums that supports topological evolution. There is also the functional approach by Turk et al. [10] utilizing radial-basis functions. Functional methods can generate intermediate shapes easily even between key shapes of different topology type. However, there is a serious problem in functional methods. The shape interpolation is applied without defining or using any topological information. As a result, time values of topological changes cannot be detected. Therefore, it is difficult to identify the time intervals for expected key frames of animation, and information on the types of topological evolution is missing. The simple interpolation between defining functions of the initial shape and the target shape is advantageous for its simplicity, and we want to make full use of this. However, as we have just seen, it has a serious drawback. To overcome this dilemma, we propose the enhanced functional method below.

Our new technique involves classification and detection of critical points. We focus on functional shape metamorphosis in its simplest form of the linear interpolation between defining functions. In function representation (FRep), geometric solids are defined by inequalities $F(X) \geq 0$, where F is an explicit real function of point coordinates X [7]. In addition, we use the R-functions, which provide analytical definitions of set theoretic operations [7]. The entire metamorphosis is defined by homotopy functions on the closed time interval $I = [0, 1]$.

The remainder of this paper is organized as follows. Section 2 reviews related work on topological analysis and shape metamorphosis with topological handles. In Sect. 3, we present a new method of detection and classification of linear shape metamorphosis based on Morse theory. Section 3 also includes a comparison with conventional Morse theory analysis and the classification of types of topological evolution. In Sect. 4, several case studies in 2D and 3D spaces are presented. In Sect. 5, we conclude the paper and discuss future work.

2 Related work

2.1 Topological analysis

There is a variety of techniques for topological analysis. The best-known method is to calculate the genus of objects. On the basis of triangulation of the object surface, one can calculate the Euler characteristic using the number of vertices V, edges E, and faces F. The Euler characteristic $e(X^3)$ is calculated by

$$e(X^3) = V - E + F,$$

which is known to be a topological invariant. The number of handles known as the genus can be obtained as:

$$p = \frac{2 - e(X^3)}{2}.$$

Another topology analysis method is based on critical points, which are defined as the zeros of the gradient of the local height function f:

$$\nabla f(X) = (f_x(X),\, f_y(X),\, f_z(X)),$$

where $f_x = \frac{\partial}{\partial x} f$. The authors of [4, 8] use critical points of 3D shapes for topological analysis. The procedure for specific skeleton-based implicit surface models [11] is an example of the critical points detection. It uses the spatial coherence of the skeleton elements to give a good first guess for the locations of the critical points.

Then, each critical point is classified according to the signs of the three eigenvalues $l_1 \leq l_2 \leq l_3$ of the Hessian, which is defined as the Jacobian of the gradient. If all three eigenvalues are not zero, the critical point is called non-degenerate and can be a maximum (peaks), minimum (pits) or some kind of saddle point. In 3D space, saddle points are classified into 1-saddle points and 2-saddle points. Table 1 indicates this classification.

Table 1. Classification of critical points based on the signs of eigenvalues of the Hessian

l_1	l_3	l_3	Critical point type
−	−	−	Maximum point
−	−	+	2-saddle point
−	+	+	1-saddle point
+	+	+	minimum point

Furthermore, the critical point type and change of the sign of the function value at the critical point are used for the classification of types of topological changes in 3D, as is shown in [8]. Our approach is close to this, but is oriented towards detection and classification of the critical points and the time values of topological evolution for shape metamorphosis.

2.2 Shape metamorphosis with topological handles

There are also methods of topological analysis using Reeb graphs [1]. The Reeb graph represents the topological skeleton of an object. Contours of the object together with the Reeb graph represent the entire 3D object. By using this method, the metamorphosis can be presented by transitions between the different topology types. There are methods of shape metamorphosis that need topological handles to be introduced between key shapes of different topology [2, 9].

Pizzanu et al. [2] proposed a method for generation of the intermediate shapes at the time values of topological evolution by using the Reeb graph and contours of objects. The topological changes are defined by the Reeb graph and the key shapes of the metamorphosis are interpolated smoothly via the time values of the topological changes. The authors of [9] classify possible topological transitions and show that for two given source and destination shapes there are several possible types of transition. Each transition type of surface topology can be controlled explicitly by introducing an additional key shape, which bridges the topological difference of two input shapes. In this method, user intervention is required during the specification of topological transition and the composition of the key shapes.

3 Critical point detection and classification

For functional methods, the initial and target shapes of a shape metamorphosis are first defined and then are interpolated by transformation functions, namely by homotopy functions such as linear interpolation on the closed interval $I = [0, 1]$.

3.1 Detection of critical points

We discuss two methods for the detection of critical points and time values called the time values of topological evolution. Both methods are based on Morse theory. The first one is a conventional Morse analysis and the second one is our newly proposed augmented Morse function analysis.

3.1.1 Conventional Morse theory analysis

The first method uses conventional Morse theory analysis. The procedure of this analysis is described below.

1. Define an initial shape and a target shape in an N-dimensional geometric space.
2. Define a homotopy function for the shape metamorphosis in an $N+1$-dimensional-space-time.
3. Create the height function from the homotopy function in an $N+1$-dimensional space-time.
4. Detect the critical points of the height function.
5. Detect the critical values when the topology changes.

In the first step, an initial shape and a target shape are defined as the key shapes of a shape metamorphosis. These key shapes can have different topology types.

In the second step, the $N+1$-dimensional (time-dependent) object is generated by a homotopy function. The homotopy function is used for generation of an $N+1$-dimensional shape metamorphosis between the N-dimensional initial $f_{ini}[x_1, x_2, \ldots, x_n]$ and the target shapes $f_{tar}[x_1, x_2, \ldots, x_n]$, which are defined as FRep models in the last step. The additional coordinate is time value, and the intermediate shapes, cross-sections of $N+1$-dimensional shape metamorphosis, can be generated automatically along the time axis by using the homotopy function. We define the homotopy function $f[x_1, x_2, \ldots, x_n, t]$ as the following linear homotopy function in the closed time interval:

$$f[x_1, x_2, ..., x_n, t] = f_{ini}[x_1, x_2, ..., x_n] \cdot (1-t) + f_{tar}[x_1, x_2, ..., x_n] \cdot t$$

In the third step, we create the height function h by expressing the time variable in terms of point coordinates as $t = h[x_1, x_2, \ldots, x_n]$. The following height function is defined in $N+1$-dimensional space and has N variants.

$$t = h[x_1, x_2, \ldots, x_n] = \frac{f_{ini}[x_1, x_2, \ldots, x_n]}{f_{ini}[x_1, x_2, \ldots, x_n] - f_{tar}[x_1, x_2, \ldots, x_n]}.$$

In the next step, we detect the critical points of the height function. The critical points are special points, where the gradient of the height function vanishes:

$$\nabla h[x_1, x_2, ..., x_n] = \left(\frac{\partial}{\partial x_1} h, \frac{\partial}{\partial x_2} h, \ldots, \frac{\partial}{\partial x_n} h \right) = 0.$$

After the detection of the critical points, the final step is only to assign the coordinate values of the critical points as the argument of the height function and thus to calculate the critical values for the topological evolution in the shape metamorphosis.

3.1.2 Augmented Morse analysis

In this section, we present our augmented Morse analysis, which is also based on Morse theory. The proposed procedure is described below.

1. Define an initial shape and a target shape in an N-dimensional geometric space.
2. Define a homotopy function for the shape metamorphosis in an $N+1$-dimensional space-time.
3. Create the height function from the homotopy function in an $N+2$-dimensional space with geometric space, time, and functional coordinates.
4. Detect critical points and time values of the height function.

In this method, the first and second steps are the same as in the conventional Morse analysis. In the third step, we introduce a different height function in a space-time with an additional dimension. The height function h is defined in an $N+2$-dimensional space, and the homotopy function defining the entire shape metamorphosis is considered a time-dependent height function:

$$h = f[x_1, x_2, \ldots, x_n, t].$$

The additional coordinate is a function value.

In the last step, we detect the critical points and time values of topological changes, on the particular function level. The values of the detected critical points and time value include the information of the coordinates as to when and where topological evolution takes place. We focus on the critical points located on the surface of some intermediate shapes. Therefore, only analysis of the particular height level where the height function equals zero is performed. We keep the zero level and analyze how the critical points appear at this level in time. Therefore, the critical points and time values have to satisfy the following conditions:

$$\frac{\partial}{\partial x_1}h = \frac{\partial}{\partial x_2}h = \ldots = \frac{\partial}{\partial x_n}h = 0$$

and

$$h = f[x_1, x_2, \ldots, x_n, t] = 0,$$

where t is a time variable and x_i are geometric point coordinates.

The condition $h = 0$ is added for analysis of only the particular height level. Note that this method is simpler than the method based on conventional Morse theory. The reason is that the complicated transformations of the expressions for representing the time as the height function are not necessary in our method.

3.2 Comparison with the conventional method

In this section, we present a comparison of conventional Morse analysis and our augmented Morse analysis. In general, we transform the expression for representing the height when we create a height function from the metamorphosis function. Therefore, it depends on what is regarded as a height. Our height function does not depend on the height axis, however, we add a function value as a height function value and the function defining entire shape metamorphosis is considered as a time dependent height function. In addition, the proposed method can perform faster than conventional Morse analysis. We benchmarked the speed of critical point detection for a typical shape metamorphosis from a torus $f_{ini}[x, y, z]$ to the union of two spheres $f_{tar}[x, y, z]$ by using the software Mathematica®. For defining the target shape, the union of two spheres, we use the R-functions, which provide analytical definitions of set theoretic operations [7]. The input data of key shapes of the shape metamorphosis are shown below, and we apply the linear metamorphosis function to them as defined earlier.

$$\begin{aligned} f_{ini}[x, y, z] &= -x^4 - 2x^2 \cdot (-1 + (-4 + y) \cdot y + z^2) \\ &\quad - (15 + (-8 + y) \cdot y + z^2) \cdot (-1 + y^2 + z^2), \\ f_{tar}[x, y, z] &= -2 \cdot (3 + x^2 + y^2 + z^2) \\ &\quad + \sqrt{2} \cdot \sqrt{x^4 + (3 + y^2 + z^2)^2 + 2x^2 \cdot (11 + y^2 + z^2)}\,. \end{aligned}$$

Table 2. The performance of the dual CPU computer used for the benchmark of the speed of critical point detection

CPU	Memory
Intel® (2.40 GHz) Pentium®4 (2.41 GHz)	512 MB RAM

In addition, we used a dual CPU computer for this estimation. For the reference, the performance of the CPU and memory used in this test are shown in Table 2.

According to this estimation of the speed of critical point detection, conventional Morse analysis takes 43.046 s, and our proposed method, the augmented Morse analysis, takes only 1.062 s. In other shape metamorphosis examples, we obtained the same results showing our proposed method is faster than conventional Morse analysis. The main problem of conventional Morse theory analysis is that it considers time as a height function and thus requires complicated transformations for representing the time variable as a function of other variables (see Sect. 3.1.1). Since our method considers the linear homotopy function as the time-dependent height function, such complicated transformations are not necessary (see Sect. 3.1.2).

3.3 Classification of critical points

After critical points have been detected, we classify them into different types. The types of critical points are maximum point, minimum point, and saddle point types. In addition, the saddle point is divided into 1-saddle point and 2-saddle point types in 3D shape metamorphosis. The classification of a critical point is used for identifying the type of topological evolution. For the classification of critical points, we calculate the Hessian H called the stability matrix in the catastrophe theory.

$$H_n = \begin{bmatrix} f_{x_1x_1} & f_{x_1x_2} & \cdots & f_{x_1x_n} \\ f_{x_2x_1} & f_{x_2x_2} & \cdots & f_{x_2x_n} \\ \vdots & \vdots & \ddots & \vdots \\ f_{x_nx_1} & f_{x_nx_2} & \cdots & f_{x_nx_n} \end{bmatrix},$$

where $f_{x_1x_1} = \frac{\partial^2}{\partial x_1 x_1} f$.

Since $f_{x_ix_j}$ equals $f_{x_jx_i}$, the stability matrix is symmetric. Then, let the leading principal minor of the Hessian be

$$Q(r) \quad (r = 1, 2, \ldots, n).$$

We can classify the critical points by using the determinant of the leading principal minor, $\det Q(r)$, without the complex calculations for the evaluation of eigenvalues, when $\det Q(r)$ does not vanish. If one of $\det Q(r)$ vanishes, the

critical point is called *degenerate*. In this paper, we consider the cases of *non-degenerate* critical points in 2D and 3D.

The critical point is classified as a saddle point when it is not a maximum point or a minimum point, and satisfies the following condition:

$$\det Q(r) \neq 0,$$

where $r = 1, 2, \ldots, n$.

In addition, as a special case, the saddle point will be classified further into two types in 3D space. We classify the saddle points into 2-saddle points or 1-saddle points by using the sign of $\det Q(3)$ in a shape metamorphosis between 3D key shapes. This is based on the fact that the product of eigenvalues equals the determinant of the matrix. If $\det Q(3)$ is positive, the critical point is classified as a 2-saddle point. If it is negative, the critical point is classified as a 1-saddle point.

Next, the critical point is classified as a minimum point, when it satisfies the following condition:

$$\det Q(r) > 0 \quad (r = 1, 2, \ldots, n).$$

Finally, the critical point is classified as a maximum point, when it satisfies the following condition:

$$(-1)^r \det Q(r) > 0 \quad (r = 1, 2, \ldots, n).$$

After the classification of the detected critical points, by using the type of the critical point and the sign of the function time derivative at the critical point, we can define how the topology changes at each critical point during the shape metamorphosis process. Table 3 shows the classification in 3D space by using the sign of the function time derivative $f_t = \frac{\partial}{\partial t} f$. There are eight types of topological evolution as shown in Table 3. When the sign of f_t at the maximum point is negative, a component disappears and we call this topological action "destroy". When the sign of f_t at the maximum point is positive, a component appears and the number of components increases. This topological action is called "create". Next, when the sign of f_t at the 2-saddle point is negative or positive, we call these topological actions "cut" or "attach/connect", respectively. When there are two disjoint components, they are attached to each other at the 2-saddle point and become a single component in the "attach/connect" action. When there is a single component, its two parts are detached from each other at the 2-saddle point and a hole is created between them by this topological "cut" action. The action of "cut" is an inverse of "attach/connect". When the sign of f_t at the 1-saddle point is negative, we call this topological action "pierce" and a hole is pierced in a component. When the sign of f_t at 1-saddle point is positive, a hole is filled and we call this action "spackle". When the sign of f_t at the minimum point is negative, a "pocket of air" is generated inside a component and this action is called "bubble".

Table 3. Correspondence between the type of critical point, sign of f_t, and action type of topological evolution

Critical point type	Sign of f_t	Action type
Maximum point	−	destroy
Maximum point	+	create
2-saddle point	−	cut
2-saddle point	+	attach/connect
1-saddle point	−	pierce
1-saddle point	+	spackle
Minimum point	−	bubble
Minimum point	+	burst

The sign of the function time derivative of the height function affect the topology at the detected critical point.

Finally, when the sign of f_t at the minimum point is positive, an air bubble within a component is burst. The shape topology changes after all these topological actions. Some of the topological changes, such as "destroy" and "create", when a component disappears or appears, are considered not intuitive in animation and may indicate that the metamorphosis model has to be modified or changed to exclude these effects.

4 Case studies in 2D and 3D

In this section, we describe case studies in 2D and 3D spaces. Two 2D examples of shape metamorphosis are described in Sect. 4.1 Then, a 3D example of shape metamorphosis from union of two tori to a sphere is described in Sect. 4.2. All symbolic computations and illustrations of 2D and 3D examples are made using the Mathematica® software and HyperFun applet, respectively.

4.1 Examples in 2D

We use the function representation (FRep), which is a generalization of implicit surfaces, for modeling each shape. Therefore, we can apply our method to shape metamorphosis defined by a real function of point coordinates in space-time. A shape metamorphosis from a union of three disks to a single ring is defined by algebraic real functions, and from a union of two rings to a single ring it is defined by FRep using *R*-functions in Sect. 4.1.1 and in Sect. 4.1.2, respectively.

4.1.1 Analysis of implicit curves metamorphosis

Here, we consider a shape metamorphosis from three disks to a ring defined by algebraic functions as a general case. In the first step, we define the initial and target shapes. The initial shape is composed of three disks whose central points are $(-1, 4)$, $(3, -1)$, and $(3, 3)$, respectively. Then, the target shape is a ring whose central

point is $(0, 0)$. Let the three disks and a ring be named $disk_1[x, y], disk_2[x, y], disk_3[x, y]$, and $ring[x, y]$. The initial $f_{ini}[x, y]$ and target $f_{tar}[x, y]$ shapes are described below:

$$f_{ini}[x, y] = disk_1[x, y] \cdot disk_2[x, y] \cdot disk_3[x, y],$$
$$f_{tar}[x, y] = ring[x, y] = -64 + 20x^2 - x^4 + 20y^2 - 2x^2y^2 - y^4,$$

where $disk_1[x, y] = 1 - (x+1)^2 - (y-4)^2$, $disk_2[x, y] = 1 - (x-3)^2 - (y+1)^2$, and $disk_3[x, y] = 1 - (x-3)^2 - (y-3)^2$.

The key shapes, the initial and target shapes, are shown in Fig. 1.

We define the linear homotopy function $f_1[x, y, t]$ for the shape metamorphosis between these two key shapes in the next step. Then, we create a 4D height function h_1 from the homotopy function and apply our method of critical points detection. The critical points satisfy the following conditions:

$$\frac{\partial}{\partial x} h_1 = \frac{\partial}{\partial y} h_1 = 0$$

and

$$h_1 = f_1[x, y, t] = 0.$$

The detected results are as follows:

$$(x, y, t) = \left\{ \begin{array}{l} (2.92938, 0.856053, 0.857969), \\ (0.736903, 3.14850, 0.871321), \\ (-2.02914, -1.84565, 0.99927) \end{array} \right\}.$$

The intermediate shapes are shown in Fig. 2 at the critical time values. The intermediate shapes are shown in Fig. 2a–c at the critical time values with the time equal to 0.8579699, 0.871321 and 0.999270 respectively.

In the next step, we classify these critical points. All critical points of this shape metamorphosis are classified as saddle points. The Hessian H_1, H_2 and H_3 and each det $Q(r)$ are described as follows:

$$H_1 = \begin{bmatrix} -99.095 & -21.4535 \\ -21.4535 & 68.1019 \end{bmatrix},$$
$$\det Q(2) = -7208.816 < 0,$$
$$H_2 = \begin{bmatrix} 42.5293 & -45.9167 \\ -45.9167 & -95.6079 \end{bmatrix},$$
$$\det Q(2) = -6161.73 < 0,$$
$$H_3 = \begin{bmatrix} -35.6525 & -39.5309 \\ -39.5309 & -29.0481 \end{bmatrix}$$
$$, \det Q(2) = -527.054 < 0.$$

Next, for identifying the type of topological evolution, we assign the detected critical point values to the function time derivative. Each time derivative of the homotopy function at the critical points is shown below:

$$f_{1t}[2.92937, 0.856053, 0.857968] = 250.153 > 0,$$
$$f_{1t}[0.736903, 3.14849, 0.871321] = 278.150 > 0,$$
$$f_{1t}[-2.02913, -1.84564, 0.999270] = 40924.0 > 0.$$

According to these results, all critical points are classified as saddle points and the signs of the function time derivative are positive. Hence, all topological actions of this shape metamorphosis are classified as the "attach/connect" type of topological evolution. We can recognize that each disjoint component attaches to one another at each topological evolution time and finally become one component.

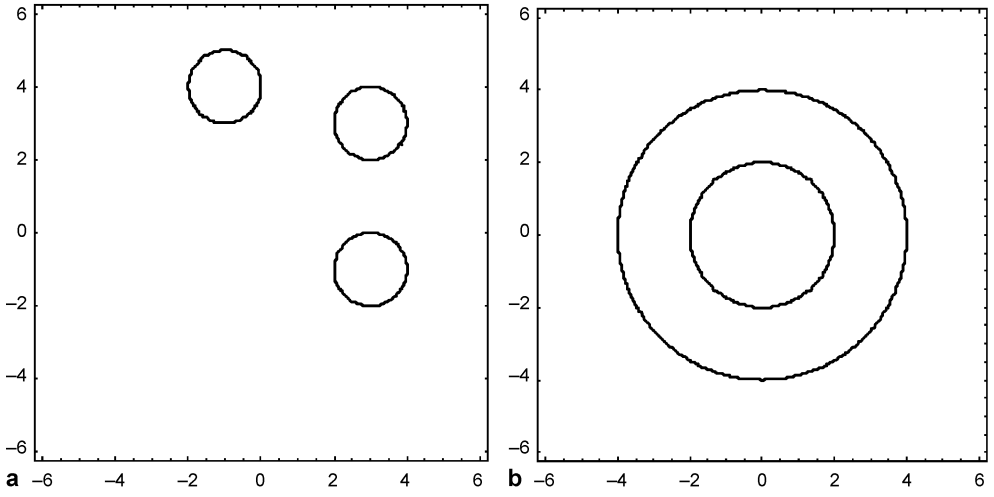

Fig. 1a,b. Initial shape **a** and target shape **b** of different topology types. **a** Union of three disks defined by using implicit curves. **b** Ring defined by using an implicit curve.

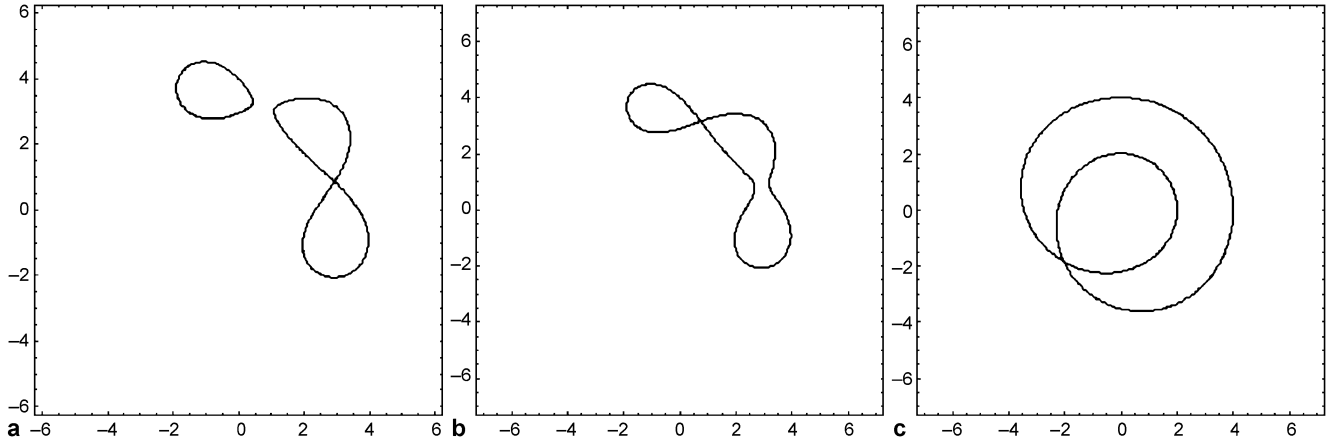

Fig. 2a–c. Intermediate shapes at the critical time values. **a** Three disjoint components become two disjoint components at the first topological evolution event. **b** Two disjoint components become one component at the second topological evolution event. **c** Both ends of the shape are attached and a hole is generated at the third topological evolution event

4.1.2 Analysis of linear FRep metamorphosis

In the previous example, the initial shape is described by pure analytical function:

$$disk_1[x, y] \cdot disk_2[x, y] \cdot disk_3[x, y].$$

However, since we need to use constructive techniques for the union, we use more general constructive FRep solid based *R*-functions [1] in this section.

Now, we consider 2D shape metamorphosis from a union of two rings to a single ring. In this metamorphosis, the initial shape and the target shape are defined by real functions $f_{ini}[x, y]$ and $f_{tar}[x, y]$. The initial shape, the union of two rings, is exactly defined by applying the *R*-function. The initial shape is the union of the ring centered at $(0, 3)$ and the one centered at $(0, -3)$, and the target shape is the ring $ring[x, y]$ used in Sect. 4.1.1. These equations of the key shapes are described below:

$$f_{ini}[x, y] = 70 - 68y^2 - 2 \cdot (x^4 + y^4 + 2x^2 \cdot (-1 + y^2)) + \sqrt{2} \cdot \sqrt{\begin{matrix} (-35 - 2x^2 + x^4)^2 \\ +4 \cdot (-559 - 141x^2 + 51x^4 + x^6) \cdot y^2 \\ +6 \cdot (133 + 70x^2 + x^4) \cdot y^4 \\ +4 \cdot (53 + x^2) \cdot y^6 + y^8 \end{matrix}},$$

$$f_{tar}[x, y] = ring[x, y].$$

In the next step, we define the linear homotopy function $f_2[x, y, t]$ for the shape metamorphosis between these two key shapes:

$$f_2[x, y, t] = f_{ini}[x, y] \cdot (1 - t) + f_{tar}[x, y] \cdot t,$$

where t is an additional time coordinate.

Then, we create a 4D height function h_2 from the homotopy function and apply our method of critical points detection. The critical points satisfy the following conditions:

$$\frac{\partial}{\partial x} h_2 = \frac{\partial}{\partial y} h_2 = 0$$

and

$$h_2 = f_2[x, y, t] = 0.$$

After the detection, the exclusion of irrelevant points is performed. The results of this method are as follows:

$$(x, y, t) = \left\{ \begin{matrix} (0, 5.67063, 0.057726), \\ (0, -5.67063, 0.057726), \\ (0, 3.19789, 0.627786), \\ (0, -3.19789, 0.627786), \\ (0, 0, 0.651221) \end{matrix} \right\}.$$

The t coordinate values of critical points are the time values when the topology changes. Other values of critical points are the geometric point coordinates where the topological evolutions take place. The entire shape metamorphosis for this example is illustrated in Fig. 3. The shapes shown in Fig. 3(b), (e) and (f) are the intermediate shapes at the critical time values equal to 0.057726, 0.627786, and 0.651221, respectively. Figure 3(c), (d) and (g) are intermediate shapes at $t = 0.1425$, $t = 0.342$ and $t = 0.75$ in this shape metamorphosis, respectively.

Then, we classify the detected critical points. We obtain the same Hessian and the classification results at the first and second critical points. The Hessians H_1 and $\det Q(r)$ at the first critical point are described as follows:

$$H_1 = \begin{bmatrix} 5.75885 & 0 \\ 0 & -63.1667 \end{bmatrix},$$

$$\det Q(2) = -363.769 < 0.$$

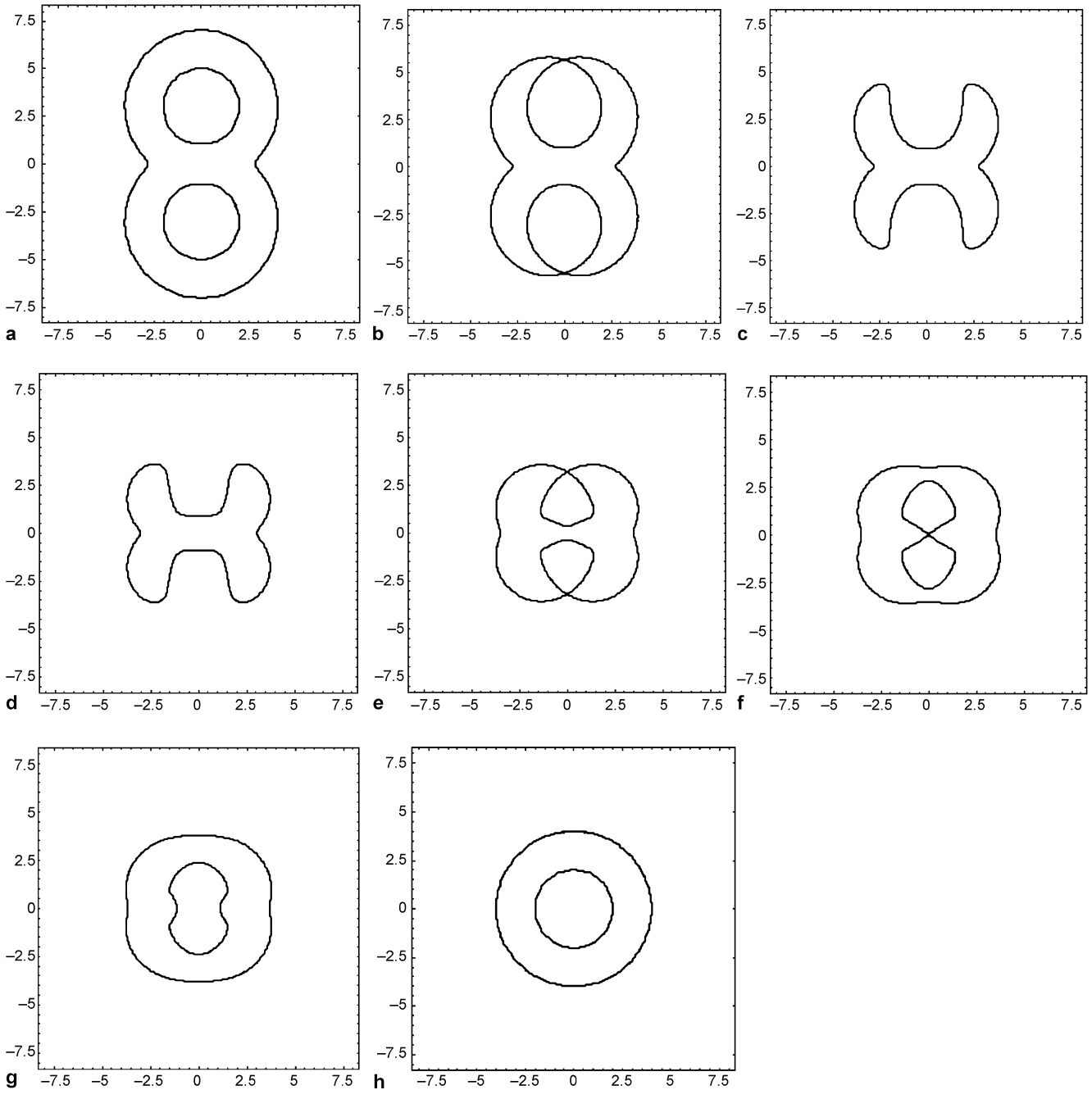

Fig. 3a–h. The sequence of shape metamorphosis from the union of two rings **a** to a ring **h**, where **b**, **e** and **f** are intermediate shapes at the detected critical time moments. The initial shape is transformed into a ring via three topological evolutions. In **b** and **e**, the two topological evolutions take place at the critical points at each time moment

Therefore, the first and second critical points are classified as a saddle point. The "cut" actions take place at these critical points, since the function time derivatives f_{2t} are negative. Similarly to the previous critical points, we apply our classification to the third and forth critical points. We also obtain the same Hessian and the classification results. The Hessian H_2 and $\det Q(r)$ at the third critical point are described as follows:

$$H_2 = \begin{bmatrix} 12.9087 & 0 \\ 0 & -36.8840 \end{bmatrix},$$
$$\det Q(2) = -476.126 < 0.$$

Therefore, the third and forth critical points are classified as saddle points. The "attach/connect" actions take place at these critical points, since the function time derivatives f_{2t} are positive. At the last critical point, we obtain the Hessian H_3 and det $Q(r)$ described as follows:

$$H_3 = \begin{bmatrix} 30.8121 & 0 \\ 0 & -52.8965 \end{bmatrix},$$
$$\det Q(2) = -1629.85 < 0.$$

Therefore, the last critical point is classified as a saddle point. The "cut" action takes place at this critical point since the function time derivative f_t is negative. Now, we can recognize this metamorphosis as a shape metamorphosis from the union of two rings to a ring with the topological evolution of "cut" and "attach".

4.2 Example in 3D

In this section, we consider the shape metamorphosis from the union of the two-tori $f_{ini}[x, y, z]$ to a sphere $f_{tar}[x, y, z]$, and the initial shape is composed with the $torus_1[x, y, z]$ and $torus_2[x, y, z]$ primitives as an FRep model based on the R-function:

$$f_{ini}[x, y, z] = torus_1[x, y, z] + torus_2[x, y, z] + \sqrt{torus_1[x, y, z]^2 + torus_2[x, y, z]^2}$$

and

$$f_{tar}[x, y, z] = 2^2 - (x-2)^2 - y^2 - z^2,$$

where $torus_1[x, y, z] = 15 - 8x^3 - x^4 - 14y^2 + 2z^2 - 8x(y^2 + z^2 - 1) - (y^2 + z^2)^2 - 2x^2(y^2 + z^2 + 7)$ and $torus_2[x, y, z] = 15 + 8x^3 - x^4 - 14y^2 + 2z^2 + 8x(y^2 + z^2 - 1) - (y^2 + z^2)^2 - 2x^2(y^2 + z^2 + 7)$.

Similarly to the previous 2D example, we also use the R-function for the union of initial shape. The initial and target shapes are shown in Fig. 4.

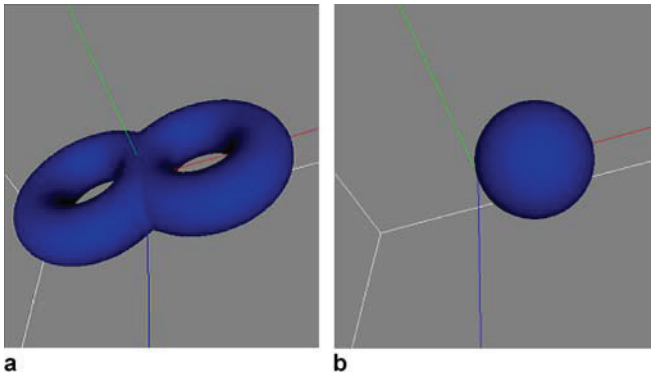

Fig. 4a,b. The initial shape **a** and the target shape **b** of different topology types

In the next step, we create the four-dimensional homotopy linear function $f_3[x, y, z, t]$ with an added time coordinate. Then, we create a 5D height function h_3 from the homotopy function and apply our method of critical points detection. The critical points satisfy the following conditions:

$$\frac{\partial}{\partial x} h_3 = \frac{\partial}{\partial y} h_3 = \frac{\partial}{\partial z} h_3 = 0$$

and

$$h_3 = f_3[x, y, z, t] = 0.$$

After detection, the exclusion of irrelevant points is performed by using a closed time interval $I = [0, 1]$. The detected critical points are described as follows:

$$(x, y, z, t) = \left\{ \begin{matrix} (-4.07456, 0, 0, 0.322143), \\ (2.04132, 0, 0, 0.683251) \end{matrix} \right\}.$$

We obtain two critical points and we can recognize that the topological evolution takes place twice in this shape metamorphosis. The intermediate shapes at the critical points shown in Fig. 5a-b are the intermediated shapes at the time values, 0.322143 and 0.683251, respectively.

In the next step, we consider the classification of the detected critical points. We create the Hessian H_1 with the assigned first critical point coordinate values, det $Q(r)$, and the function time derivative at the critical point as shown below:

$$H_1 = \begin{bmatrix} -22.4358 & 0 & 0 \\ 0 & -20.7677 & 0 \\ 0 & 0 & 1.26227 \end{bmatrix},$$
$$\det Q(2) = 465.941 > 0,$$
$$\det Q(3) = 588.124 > 0,$$
$$f_{3t}[-4.07456, 0, 0, 0.322143] = -48.5358 < 0.$$

Since det $Q(1)$ is negative, and det $Q(2)$ and det $Q(3)$ are positive, the first critical point is classified as a 2-saddle point. Moreover, the sign of the function time derivative at the first critical point is negative. Hence, the topological action "cut" takes place at the time value of the first topological evolution. Similarly, we create the Hessian H_2 with the assigned second critical point coordinate values, det $Q(r)$, and the function time derivative at the critical point as shown below:

$$H_2 = \begin{bmatrix} 4.94817 & 0 & 0 \\ 0 & -4.94455 & 0 \\ 0 & 0 & 4.41628 \end{bmatrix},$$
$$\det Q(2) = -24.4665 < 0,$$
$$\det Q(3) = -108.051 < 0,$$
$$f_{3t}[2.04132, 0, 0, 0.683251] = 12.6229 > 0.$$

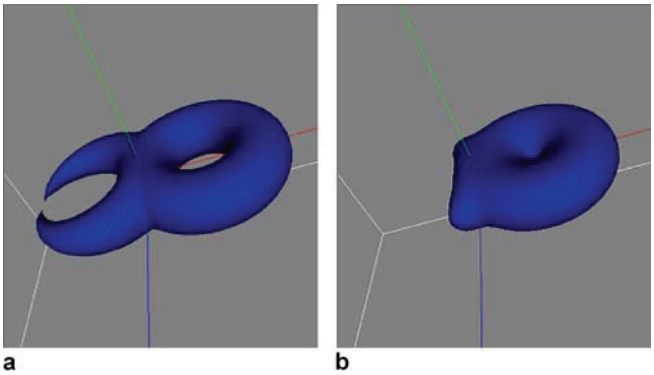

Fig. 5a,b. The intermediate shapes at the critical time moments made by the HyperFun software. **a** The genus changes at the first topological evolution event. **b** A hole is spackled at the second topological evolution event

Since det $Q(1)$ is positive, and det $Q(2)$ and det $Q(3)$ are negative, the first critical point is classified as a 1-saddle point. Moreover, the sign of the function time derivative at the second critical point is positive. Hence, the topological action "spackle" takes place at the time value of the second topological evolution.

5 Conclusion

In this paper, we presented a method of detection and classification of critical points where topological evolution takes place. In general, for functional shape metamorphosis animation, animators set the parameters of the function of the shape metamorphosis if they detect an unwanted effect. Some of the topological changes, especially "destroy" and "create", when a separate shape component disappears or appears, are considered not intuitive in animation and may indicate the necessity to improve or completely change the metamorphosis model to eliminate the detected unwanted effects. In addition, animators identify the time interval of key frames taking topological evolution into account. Although these procedures depend on the experiences of animators, our method can help solve the problems and can reduce labor hours.

By the detection of critical points and time values, we can recognize when and where topological evolution takes place. For functional shape metamorphosis animation, we can identify the time interval of special interest at the time values of topological evolution. The detected critical points can also be used for ease-in and ease-out effects in generation of intermediate shapes at critical time values of animation. In addition, we can identify the view position of the camera based on the critical point during the metamorphosis process.

The proposed method does not depend on the height axis, and complicated transformations of expressions for representing time as a height function are not necessary in our method in contrast with conventional Morse analysis. Moreover, we can identify the type of topological evolution by the detected critical point classification and the sign of the function time derivative value at the critical point. We can confirm how an initial shape changes into a target shape via topological evolutions without visual checking of the calculated metamorphosis animation or some of its frames.

In this paper, we used the linear homotopy function for shape metamorphosis. Usually, some unwanted effects take place in linear shape metamorphosis, because there is the serious limitation that key shape models have to significantly overlap. Then, we need to change the positions of the key shape models to avoid the unwanted effects recognized by our method of classification of the type of topological evolution. Alternatively, we can use non-linear shape metamorphosis instead of linear shape metamorphosis. The proposed method can also be used for the analysis of non-linear shape metamorphosis instead. The difference is only to use some non-linear function for homotopy description for the shape metamorphosis. We will apply our method to analyze non-linear shape metamorphosis and this will be a subject of future work.

References

1. Attene, M., Biasotti, S., Spagnuolo, M.: Re-Meshing techniques for topological analysis. In: Proceedings of the International Conference on Shape Modelling & Applications (SMI 2001), Italy, pp. 142–153. IEEE Computer Society, Washington, D.C. (2001)
2. DeCarlo, D., Gallier, J.: Topological evolution of surfaces. In: Proceedings of the Conference on Graphics Interface'96, Toronto, ON, Canada, pp. 194–203. Canadian Information Processing Society, Toronto, ON, Canada (1996)
3. Galin, E., Akkouche, S.: Blob metamorphosis based on Minkowski sums. Comput. Graph. Forum (Eurographics '96) **15**, 143–153 (1996)
4. Hart, J.C., Durr, A., Harsh, D.: Critical points of polynomial metaballs. In: Proceedings of Implicit Surfaces 98, Eurographics/SIGGRAPH Workshop, pp. 69–76 (1998)
5. Kanongchaiyos, P., Nishita, T., Shinagawa, Y., Kunii, TL.: Topological morphing using Reeb graphs. In: Proceedings of the First International Symposium on Cyber Worlds (CW2002), Tokyo, Japan, pp. 465–471. IEEE Computer Society Press, Los Alamitos, CA (2002)
6. Lazarus, F., Verroust, A.: Three-dimensional metamorphosis: a survey. Visual Comput. **14**, 373–389 (1998)
7. Pasko, A., Adzhiev, V., Sourin, A., Savchenko, V.: Function representation in geometric modeling: concepts, implementation and applications. Visual Comput. **11**(8), 429–446 (1995)
8. Stander, B., Hart, C.J.: Guaranteeing the topology of an implicit surface

polygonization for interactive modeling. In: Proceedings of SIGGRAPH '97, pp. 279–286. ACM Press/Addison-Wesley Publishing Co., New York, NY, USA (1997)
9. Takahashi, S., Kokojima, Y., Ohbuchi, R.: Explicit control of topological transitions in morphing shapes of 3D meshes. In: Proceedings of Pacific Graphics 2001, pp. 70–79 (2001)
10. Turk, G., O'Brien, J.: Shape transformation using variational implicit functions. In: Proceedings of the 26th Annual Conference on Computer Graphics and Interactive Techniques, pp. 335–342. ACM Press/Addison-Wesley Publishing Co., New York, NY, USA (1999)
11. Wu, S.-T., de Gomensoro Malheiros, M.: On improving the search for critical points of implicit functions. The Fourth International Workshop on Implicit Surface, ACM SIGGRAPH, Bordeaux, France, pp. 73–80 (1999)

TOMOYUKI NIEDA received the B.S. degree in Computer and Information Sciences from Hosei University in 2003. Currently, he is a graduate student in Department of Computer and Information Sciences, Hosei University, Tokyo, Japan. His research interests include computer graphiscs, shape modeling, and shape analysis.

ALEXANDER PASKO is a professor at Hosei University in Japan. He received M.Sc. and Ph.D. degrees in computer science from Moscow Engineering Physics Institute (MEPI, Russia) in 1983 and 1988. He was a researcher at MEPI from 1983 to 1992 and an assistant professor at the University of Aizu (Japan) from 1993 to 1999. His research interests include solid and volume modeling, animation, multidimensional visualization, multimedia, and computer art. He is a member of ACM SIGGRAPH, IEEE and Eurographics Association.

TOSIYASU L. KUNII is currently Professor and IT Institute Director at Kanazawa Institute of Technology, Distinguished Professor and Advisor of Beihang University in Beijing, Honorary Visiting Professor of University of Bradford in UK, and Professor Emeritus of the University of Tokyo and of the University of Aizu. He was Professor of Hosei University from 1998 to 2003. Before that he served as the Founding President and Professor of the University of Aizu dedicated to computer science and engineering as a discipline, from 1993 to 1997. He had been Professor of Department of Computer and Information Science at the University of Tokyo from June 1978 until March 1993, after serving as Associate Professor at Computer Centre of the University of Tokyo in October 1969. He was visiting professors at University of California at Berkeley in 1994 and University of Geneva in 1992. He received his B.Sc. in 1962, M.Sc. in 1964 and D.Sc. in 1967 all from the University of Tokyo. He received the 1998 Taylor L. Booth Education Award the highest education award of IEEE Computer Society given to one individual a year. He is Fellow of IEEE and IPSJ. He has published over 50 books and over 300 refereed papers in computer science. Dr. Kunii was Founder and Editor-in-Chief of The Visual Computer: An International Journal of Computer Graphics (Springer-Verlag) (1984–1999), and International Journal of Shape Modeling (World Scientific) (1994–1995), and was Associate Editor of IEEE Computer Graphics and Applications (1982–2002). He is Associate Editor-in-Chief of The Journal of Visualization and Computer Animation (John Wiley & Sons) (since 1990) and on the Editorial Board of Information Systems Journal (since 1976), and Information Sciences Journal (since 1983).